



HAL
open science

Absorption and emission spectra of U4 + diluted in the incommensurate structure of ThCl4

C. Khan Malek, J.C. Krupa, P. Delamoye, M. Genet

► **To cite this version:**

C. Khan Malek, J.C. Krupa, P. Delamoye, M. Genet. Absorption and emission spectra of U4 + diluted in the incommensurate structure of ThCl4. *Journal de Physique*, 1986, 47 (10), pp.1763-1773. 10.1051/jphys:0198600470100176300 . jpa-00210372

HAL Id: jpa-00210372

<https://hal.science/jpa-00210372>

Submitted on 4 Feb 2008

HAL is a multi-disciplinary open access archive for the deposit and dissemination of scientific research documents, whether they are published or not. The documents may come from teaching and research institutions in France or abroad, or from public or private research centers.

L'archive ouverte pluridisciplinaire **HAL**, est destinée au dépôt et à la diffusion de documents scientifiques de niveau recherche, publiés ou non, émanant des établissements d'enseignement et de recherche français ou étrangers, des laboratoires publics ou privés.

Classification
Physics Abstracts
78.40 — 78.50

Absorption and emission spectra of U^{4+} diluted in the incommensurate structure of $ThCl_4$

C. Khan Malek, J. C. Krupa, P. Delamoye and M. Genet

Laboratoire de Radiochimie, Institut de Physique Nucléaire, Université Paris-Sud, 91406 Orsay France

(Reçu le 11 avril 1986, accepté le 9 juin 1986)

Résumé. — Les spectres d'absorption et de fluorescence de U^{4+} dilué dans des monocristaux de $ThCl_4$ ont été mesurés de 4,2 K jusqu'à la température ambiante. Les cristaux de $\beta-ThCl_4$ présentent une structure incommensurable en dessous de 70 K avec une perte de la périodicité le long de l'axe c . Ceci a pour conséquence une variation de la distance métal-halogène lorsqu'on passe d'une maille à l'autre. La symétrie du site de l'ion actinide est ainsi abaissée. Les raies correspondant au site de symétries S_4 et D_2 ont été identifiées par spectroscopie. La symétrie S_4 a été ramenée à celle de D_{2d} et une analyse paramétrique des niveaux d'énergie de U^{4+} en symétrie D_{2d} et D_2 est donnée. Pour 25 niveaux dans le site D_{2d} , l'écart quadratique moyen σ est de 46 cm^{-1} et de 56 cm^{-1} pour les 34 niveaux en symétrie D_2 . Les paramètres qui interviennent dans les calculs pour les deux symétries sont légèrement différents.

Abstract. — The absorption and fluorescence spectra of U^{4+} diluted in single crystals of $ThCl_4$ have been measured at temperatures ranging from 4.2 K to room temperature. $\beta-ThCl_4$ exhibits an incommensurate structure below 70 K with a loss of periodicity along the c axis. This results in a variation of the distance between the metal and the halogen from one cell to another. The site symmetry of the actinide ions is then reduced. The lines corresponding to the sites of the resulting symmetries S_4 and D_2 are identified spectroscopically. The S_4 symmetry is approximated by the D_{2d} one and a parametric analysis of the energy levels of U^{4+} in the D_{2d} and D_2 symmetries is reported. For 25 levels in the D_{2d} site the root mean square deviation σ is 46 cm^{-1} and for 34 levels in D_2 , $\sigma = 56\text{ cm}^{-1}$. The parameters which occur in both symmetries are only slightly changed.

1. Introduction.

There has recently been some interest shown in the studies of the tetravalent uranium ion U^{4+} ($5f^2$) in solid state matrices that started with the new parametric analysis of U^{4+} in $\beta-ThBr_4$ [1] (U^{4+} at a site of D_{2d} or D_2 symmetry) followed by a reinterpretation of the spectra of U^{4+} in the borohydrides [2] with the U^{4+} ion at a site of T_d symmetry. The study of U^{4+} in $ThCl_4$ brings a new set of spectroscopic parameters for U^{4+} at a site of relatively high symmetry (D_{2d}) which can be compared to those obtained in the bromide matrix $ThBr_4$. Both matrices offer a similar dodecahedron of coordination for the U^{4+} ion and like $ThBr_4$ [3], $ThCl_4$ undergoes a second order displacive phase transition at a temperature $T_c = 70\text{ K}$. Below T_c , neutron diffraction experiments revealed that the crystal structure of $ThCl_4$ is incommensurate and modulated [4], due to

transverse displacements of the chloride ions perpendicular to the c axis of the crystals. These displacements are different in each unit cell and they can be described as in $ThBr_4$ in terms of a local phase φ_1 , where l is the index which identifies the cell [5]. The modulation reduces the site symmetry of the actinide ion that is D_{2d} at room temperature and S_4 , D_2 , C_2 at low temperature, according to the φ_1 values :

for $\varphi_1 = 0$, the symmetry of the site is S_4 ,

for $\varphi_1 = \pm \pi/2$, the U^{4+} sites are described by the D_2 symmetry,

for $0 < |\varphi_1| < \pi/2$, the sites are described by the C_2 symmetry.

There exists a continuous variation of the environment, thus of the crystal field around the U^{4+} ion and consequently the energy levels of U^{4+} are modulated between two extreme positions corresponding to $\varphi_1 = 0$ and $\varphi_1 = \pm \pi/2$ for a π band and $\varphi_1 = \pm \pi/2$ for a σ band. The shapes of these bands

are then characteristic (Fig. 1). They are described by the model of Delamoye and Currat [5] as a continuum of lines limited by two sharp edges. They correspond to the sites of D_2 symmetry (σ band) or S_4 and D_2 symmetries for a π band. Site selective excitation of the U^{4+} absorption levels permitted us to correlate the absorption and emission lines [6] and in particular to identify transitions of U^{4+} ions at sites of D_2 and S_4 symmetries. Therefore we are in a position to analyse the U^{4+} energy levels in these both sites.

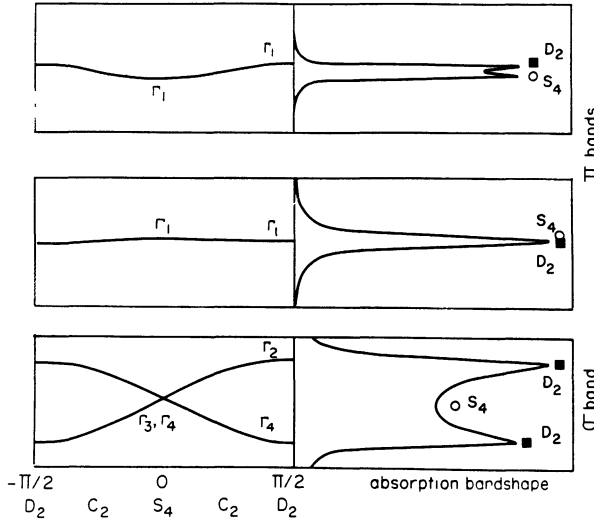


Fig. 1. — U^{4+} absorption bandshapes in the incommensurate structure of $ThCl_4$.

2. Experimental details and analysis of the data.

β - $ThCl_4$ single crystals were grown by the Bridgman method [7]. The crystal structure is tetragonal [8] space group $I4_1/amd$ at room temperature (β form of $ThCl_4$ [9]). $ThCl_4$ was doped with about 0.1 % of U^{4+} , the doping material being UO_2 or UCl_4 . The crystals were cleaved and polished in a dry box because of their hygroscopicity and they were sealed under a helium atmosphere (300 torrs) in silica tubes. The crystals used for the measurements were about $15 \times 3 \times 5 \text{ mm}^3$ or smaller. They presented a cleavage face which was not exactly perpendicular to the fourfold axis so they can be oriented in order to take polarized spectra σ and $\sigma + \pi$. Experiments at low temperature were performed in an Oxford Instruments helium gas circulating cryostat.

The absorption and emission spectra were recorded at different temperatures between 4.2 K and 300 K in the visible and infrared region ($0.3 \mu\text{m} - 2.5 \mu\text{m}$) on a one meter HR 1000 Jobin Yvon spectrometer. It is equipped in the visible region with a 1200 lines/mm grating and a photomultiplier, and in the infrared with a 600 lines/mm and a PbS detector. The calibration

was made with a low pressure mercury lamp before and after the recording of the spectrum. Fluorescence spectra were excited with a Sopra nitrogen pumped dye laser.

The surrounding of the U^{4+} ions in the different symmetries mentioned before is non-centrosymmetric (non-inversion centre), so strong zero phonon transitions are expected. All spectra were analysed with a linear polarizer which can be oriented in both parallel and perpendicular directions relative to the C_4 optical axis which is preserved below the phase transition temperature in the tetragonal structure of the incommensurate phase. The σ and α spectra were checked to be identical, thus leaving us only with electric dipole transition to deal with. Though the polarization is expected to be complete (π or $\sigma(\alpha)$) (for definition see Table I), the $\sigma + \pi$ were recorded instead of the pure π spectra, which is due to a slight misorientation regarding the C_4 axis on the various crystals that were studied.

Table I. — Electric dipole selection rules in the D_{2d} (a), S_4 (b) and D_2 (c) symmetries, notations from Nielson and Koster [11]. A σ polarization corresponds to a spectrum recorded with the electric field E perpendicular to the principal axis C_4 whereas a π spectrum corresponds to E parallel to this axis.

D_{2d}	Γ_1	Γ_2	Γ_3	Γ_4	Γ_5
Γ_1				π	σ
Γ_2			π		σ
Γ_3		π			σ
Γ_4	π				σ
Γ_5	σ	σ	σ	σ	π

S_4	Γ_1	Γ_2	Γ_3, Γ_4 (*)
Γ_1		π	σ
Γ_2	π		σ
Γ_3, Γ_4 (*)	σ	σ	π

(*) Γ_3 and Γ_4 are pseudo-degenerate levels (same energy).

D_2	Γ_1	Γ_2	Γ_3	Γ_4
Γ_1		σ	π	σ
Γ_2	σ		σ	π
Γ_3	π	σ		σ
Γ_4	σ	π	σ	

Some 75 % of the lines can be seen with the σ polarization and the lines observed with a π polarization are generally weaker than those with a σ polarization (Fig. 2). This trend has also been seen on $ThSiO_4 - U^{4+}$ [10] where the U^{4+} ion is at a site of D_{2d} symmetry as well. The lines in β - $ThCl_4 - U^{4+}$ with a polarization σ are in general

broader than those with the polarization π . This has been explained by the Delamoye and Currat's analysis [5] of the line shapes recorded in β -ThBr₄-U⁴⁺. The width of the lines in ThCl₄-U⁴⁺ are broader overall than those in ThSiO₄-U⁴⁺ which offers a regular D_{2d} site for U⁴⁺ at low temperature.

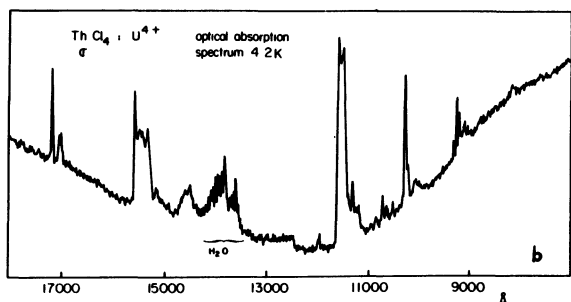
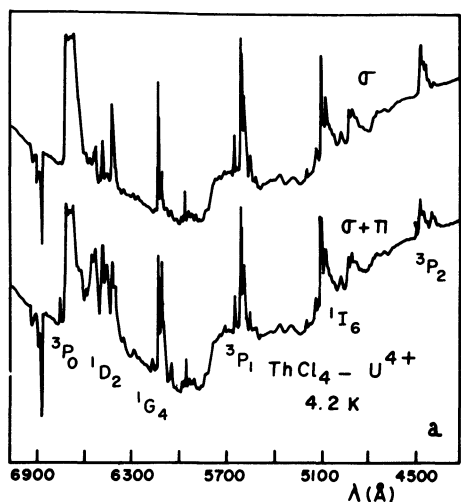


Fig. 2. — Absorption spectra of ThCl₄-U⁴⁺ in the visible (a) and IR (b).

Although in the modulated structure of β -ThCl₄ the symmetry of the actinide site is lowered ($S_4 - C_2 - D_2$), we shall use the D_{2d} designation in the labelling of the energy levels. It can be noted that the electric dipole selection rules for the D_{2d} and S₄ (subgroup of D_{2d}) groups [11] only differ for the transitions (Table I):

$$\begin{aligned} \Gamma_3 &\leftrightarrow \Gamma_1 \\ & \quad (D_2) \\ \Gamma_2 &\leftrightarrow \Gamma_4 \end{aligned}$$

that are forbidden in the D_{2d} symmetry and allowed with a π polarization in the S₄ symmetry as $\Gamma_1 \rightarrow \Gamma_2$ transitions.

The other selection rules are the same.

In the S₄ symmetry the loss of symmetry elements is responsible for the introduction of imaginary terms in the crystal field hamiltonian, Im B₄⁴ and Im B₆⁶, whereas all the crystal field parameters are real in the D_{2d} symmetry (Table II). Interpreting the data in the D_{2d} symmetry instead of in the S₄ symmetry results in neglecting these imaginary terms in the even rank crystal field components that are used for the calculations of the energy levels of the optically active ions. Nevertheless the use of the D_{2d} symmetry in place of the S₄ symmetry should give us the main features of the spectra. Esterowitz *et al.* [12] had already noticed with Pr³⁺ doped in LiYF₄ at a site of S₄ symmetry that the use of the D_{2d} selection rules was a good approximation in identifying energy levels. Hence the D_{2d} symmetry will be considered in our case. The crystal field eigenstates carry the Γ_1 through Γ_5 irreducible representations associated with the D_{2d} site symmetry. Only the Γ_5 representation is doubly degenerate, the remaining Γ_1 to Γ_4 being non degenerate. The lowering of the symmetry from D_{2d} to D₂ lifts the degeneracy of the Γ_5 levels of energy. Thus there are only singlets carrying the Γ_1 to Γ_4 point group representations associated with the D₂ symmetry. The correspondance between the sets of representations are in the D_{2d}, S₄ and D₂ symmetries shown in table III. The selection rules for the electric dipole transitions for the D_{2d} and D₂ symmetries are given in the table I.

Table II. — Crystal field parameters of even rank in the D_{2d} (a), S₄ (b) and D₂ (c) symmetries.

a) D _{2d} symmetry	b) S ₄ symmetry	c) D ₂ symmetry
B ₀ ² , B ₀ ⁴ , B ₀ ⁶	B ₀ ² , B ₀ ⁴ , B ₀ ⁶	B ₀ ^{2'} , B ₂ ^{2'}
B ₄ ⁴ , B ₄ ⁶	B ₄ ⁴ + iB ₄ ⁴	B ₀ ^{4'} , B ₂ ^{4'} , B ₄ ^{4'}
	B ₄ ⁶ + iB ₄ ⁶	B ₀ ^{6'} , B ₂ ^{6'} , B ₄ ^{6'} , B ₆ ^{6'}

Table III. — Correspondence between the sets of representations in the D_{2d}, S₄ and D₂ symmetries [11].

D _{2d}	S ₄	D ₂
Γ_1	Γ_1	Γ_1
Γ_2	Γ_1	Γ_3
Γ_3	Γ_2	Γ_1
Γ_4	Γ_2	Γ_3
Γ_5	$\Gamma_3 + \Gamma_4$	$\Gamma_2 + \Gamma_4$

Following the study of U⁴⁺ in β -ThBr₄ on which Zeeman and M.C.D. studies were performed [13], the ground state level is assumed to be a (D_{2d}) Γ_4 level, which is consistent with our interpretation of

the crystal field transitions. At 4.2 K the σ lines correspond to transitions from the $(D_{2d}) \Gamma_4$ ground state to the doubly degenerate $(D_{2d}) \Gamma_5$ levels of energy while the lines recorded with the π polarization correspond to transitions to the $(D_{2d}) \Gamma_1$ non degenerate levels of energy.

In the most intense peaks a contribution of U^{4+} ions at a site of D_{2d} symmetry is expected. Indeed the intensity of the electric dipole transitions in the same configuration and regardless of the site symmetry of the ion, is proportional to matrix elements involving the crystal field parameters of odd rank $(B^{*k} q)^2$.

The D_2 symmetry is close to the D_{2d} symmetry at low temperature so the additional parameters $B_4^{*5'}$, $B_4^{*7'}$ and $B_6^{*7'}$ to be added to the odd rank parameters for the D_{2d} symmetry (B_2^{*3} , B_2^{*5} and B_2^{*7}) can be supposed to be weak. Therefore the intensity of the lines corresponding to the U^{4+} ions in the D_{2d} and D_2 symmetries will follow the same trend.

There are more lines than are theoretically expected from a Γ_4 ground state, even if some additional lines are assumed to come from U^{4+} ions at sites of D_2 and C_2 symmetries alone according to the selection rules. Some lines are vibronic in origin and they are found on the blue side of the electronic lines at 4.2 K. When excited they give the same fluorescence spectra as the electronic lines they are associated with. Some other lines are probably due to an impurity or to U^{3+} . In β - $ThBr_4 - U^{4+}$, M.C.D. experiments [13] showed an anomalously high g value for certain lines that are attributed to impurities.

At higher temperature transitions from a low-lying level at 55 cm^{-1} are readily apparent. This level has also been seen in fluorescence experiments [6]. It can be interpreted as a D_2 level arising from the splitting of the first excited Stark level represented by Γ_5 in the D_{2d} symmetry. The shape of the bands in β - $ThCl_4 - U^{4+}$ is modified when the temperature is increased (Fig. 3). In particular the sharp edges corresponding to transitions of the U^{4+} ions at sites of D_2 symmetry decrease in intensity. Those edge singularities finally disappear and the D_{2d} line is left alone at 70 K. With increasing concentration of U^{4+} a decrease in the sharp edges is also observed.

The fluorescence spectrum of U^{4+} in the solid state is reported here for the third time. It had already been exhibited in $ThBr_4 - U^{4+}$ [14] and in $Cs_2ZrBr_6 - U^{4+}$ [15]. At 4.2 K with the halogen lamp as excitation source two broad features at 5131 Å and 6870 Å are observed. They correspond to the radiative transitions between the levels: $^1I_6 \rightarrow ^3H_4$ and $^1D_2 \rightarrow ^3H_4$ respectively. Those emission

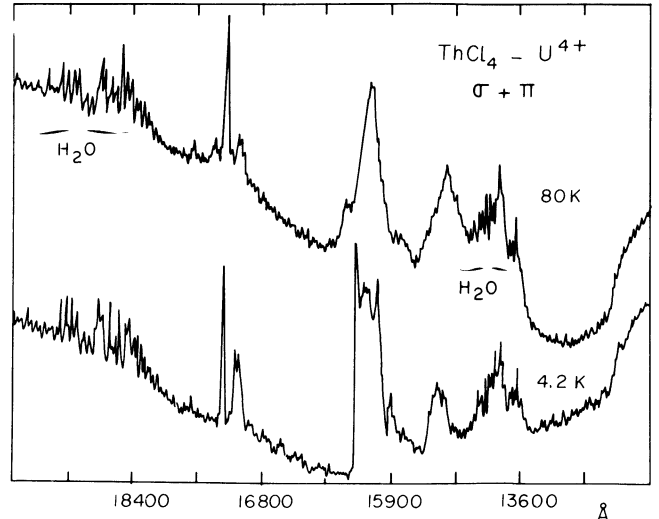


Fig. 3. — Absorption spectra of $ThCl_4 - U^{4+}$ above and below the phase transition temperature.

lines are strongly dependent on temperature and the energy of the exciting radiation. The results of some site selective excitation experiments at 4.2 K are given in table IV, with their assignment.

Dye laser excitation experiments were performed in the absorption bands in the visible region in order to identify the lines corresponding respectively to the D_{2d} and D_2 symmetries. Indeed, the induced green and red fluorescence permitted us to correlate the observed transitions and attribute a definite symmetry to the U^{4+} from which they originate [6]. In the I.R. region where no fluorescence was observed, the middle of the absorption band was taken as corresponding to the D_{2d} both in the σ and π spectra. The levels to be taken into account in the I.R. for the D_2 symmetry are the limiting lines of the bands in the σ spectrum and the middle of the bands in the π spectrum. The error committed by doing so should not be very large, at least in the spectra where the π lines are much narrower than those observed in the σ polarization [5].

3. Calculations and discussion.

The levels were fitted by simultaneous diagonalization of the free ion, \hat{H}_0 , and crystal field Hamiltonians $\hat{H}_{cc} + \hat{H}'_{cc}$ [16]:

$$\hat{H} = \hat{H}_0 + \hat{H}_{cc} + \hat{H}'_{cc}$$

where \hat{H}_0 is characterized by the parameters of:

- interelectronic repulsion F^k , $k = 2, 4, 6$
- spin-orbit coupling ζ
- configuration interaction α , β and γ

plus the P^k ($k = 2, 4, 6$) and M^k ($k = 0, 2, 4$) parameters describing respectively the electrostatically correlated spin-orbit (P^k), spin-spin and spin-other orbit (M^k) interactions.

Table IV. — Emission spectrum of $ThCl_4 - U^{4+}$ at 4.2 K.

a) 000, 00, 0 : strong lines in order of decreasing intensity.

b) ***, **, * : very weak lines in order of decreasing intensity.

D_{2d} $\lambda_{exc} = 5\ 112.1\ \text{\AA}$ (19 556 cm^{-1})		D_2 $\lambda_{exc} = 5\ 116.5\ \text{\AA}$ (19 539 cm^{-1})	
\AA	cm^{-1}	\AA	cm^{-1}
$^1D_2 \rightarrow ^3H_4$			
000 6 896	14 498	000 6 870	14 552
00 6 931	14 424	0 6 899	14 491
** 6 945	14 395	00 6 930	14 426
* 6 974	14 335	* 6 955	14 374
** 6 982	14 319	* 6 974	14 335
* 6 994	14 294		
* 7 207	13 872	*** 7 216	13 854
$^1I_6 \rightarrow ^3F_2$			
** 6 519	15 336	* 6 515	15 345
		** 6 543	15 279
* 6 536	15 296	* 6 563	15 233
* 6 565	15 228	** 6 603	15 140
** 6 610	15 124	** 6 610	15 124
$^1I_6 \rightarrow ^3H_4$			
		0 5 116	19 541
000 5 142	19 444	000 5 131	19 484
0 5 147	19 423	0 5 146	19 427
*** 5 378	18 589	0 5 151	19 408
** 5 383	18 572	** 5 386	18 561
** 5 433	18 401	* 5 438	18 384
** 5 464	18 297		
** 5 519	18 114		

\hat{H}_{cc} corresponds to the crystal field Hamiltonian that includes the parameters of the same rank k and multiplicity q for the D_{2d} and D_2 symmetries. The supplementary parameters to be added in the case of the D_2 symmetry are taken into account in \hat{H}'_{cc} , which is considered to be a perturbation of \hat{H}_{cc} , due to the low magnitude of the crystal field modulation. $B_0^2, B_0^4, B_4^4, B_0^6$ and B_4^6 , parametrize the action of \hat{H}_{cc} in the D_{2d} symmetry, and $B_0^2, B_0^4, B_4^4, B_0^6$ and B_4^6 parametrize the main effect of \hat{H}_{cc} in the D_2 symmetry, with the perturbation to the lowering of symmetry being taken into account by the additional D_2 parameters B_2^2, B_2^4, B_6^6 on which is built \hat{H}'_{cc} .

4. Fitting in the D_{2d} and D_2 symmetries.

4.1. D_{2d} SYMMETRY CALCULATIONS. — The starting values for the various parameters were taken from U^{4+} in $\beta - ThBr_4$ [1] and the B_q^k were varied till a reasonable fit was obtained. Then both the free ion parameters F^k and ζ , and the crystal field parameters B_q^k were varied. In a last step the configuration interaction parameters α and β were allowed to vary but the parameter γ was fixed at the value found in $ThBr_4 - U^{4+}$ [1], because the position of the 1S_0 which fixes, with the 3P_0 , the γ value is not known. The P^k and M^k were left as well at the values in $ThBr_4 - U^{4+}$.

An r.m.s. deviation σ of 46 cm^{-1} was obtained for 25 experimental levels. The spectroscopic parameters corresponding to this last fit are listed in table V and the observed and calculated energy levels along with the U^{4+} eigenvectors in the D_{2d} symmetry are given in table VI. This table shows the fluorescing level of the singlet 1I_6 above the energy gap $^1I_6 - ^3P_1$. However the agreement between the experimental and calculated levels is overall satisfactory.

4.2. D_2 SYMMETRY CALCULATIONS. — Since the effects of the incommensurate structure which lowers the symmetry from D_{2d} to D_2 are presumed to be small, we adopted the same procedure as was used for $ThBr_4 - U^{4+}$ [1] in order to determine the D_2 crystal field parameters. In a first step, the D_2 levels were treated as D_{2d} by fixing the F^k and ζ parameters and fitting those which are common to D_{2d} and D_2 symmetries to the (D_2) Γ_1 levels and to the centers of gravity of $\Gamma_2 - \Gamma_4$ pairs (Γ_5 in D_{2d}). Then each experimental $\Gamma_2 - \Gamma_4$ pair was adjusted to reproduce the calculated centers of gravity so that the variation of the B_q^k parameters would fit only the $\Gamma_2 - \Gamma_4$ splitting. With these parameters as initial values, the Slater parameters, the spin-orbit constant ζ , and all of the crystal-field parameters were allowed to vary.

For 34 levels, the r.m.s. deviation was 56 cm^{-1} . The parameters (Table V) common to D_{2d} and D_2 symmetries have close values and the additional parameters are all small in both symmetries. The results are reported in tables V and VII.

5. Discussion.

We used the crystal field model to successfully interpret the energy levels of U^{4+} in the sites of approximate D_{2d} and D_2 symmetry in the incommensurately modulated structure of $\beta - ThCl_4$. Both the large spin-orbit and crystal field interactions result in an effective J -mixing in the U^{4+} eigenvectors. The Auzel and Malta's parameter [17]:

$$\frac{N_v}{\sqrt{4\pi}} = \left(\sum_k \frac{1}{2k+1} (B_q^k)^2 \right)^{1/2}$$

Table V. — Spectroscopic parameters of U^{4+} (in cm^{-1}) — the r.m.s. deviation σ is :

$$\sigma = \left(\sum_i (E_{obs.}^i - E_{calc.}^i)^2 / n - m \right)^{1/2}$$

— Uv : free ion— U^{4+} : in the borohydrides in T_d symmetry— U^{4+} in ThX_4 in D_{2d} and D_2 symmetrieswhere n is the number of observed levels and m the number of parameters varied.

Spectroscopic parameters	Uv (19)	in D_{2d} symmetry			in D_2 symmetry	
		$U(BD_4)_4$ in $Hf(BD_4)_4$ (2)	$ThBr_4 - U^{4+}$ (1)	$ThCl_4 - U^{4+}$	$ThBr_4 - U^{4+}$ (1)	$ThCl_4 - U^{4+}$
F^2	$51\,938 \pm 39$	$41\,121 \pm 236$	$42\,253 \pm 127$	$42\,752 \pm 162$	$42\,264 \pm 84$	$42\,736 \pm 175$
F^4	$42\,708 \pm 100$	$38\,849 \pm 1\,071$	$40\,458 \pm 489$	$39\,925 \pm 502$	$41\,159 \pm 407$	$39\,821 \pm 589$
F^6	$27\,748 \pm 68$	$21\,711 \pm 827$	$25\,891 \pm 383$	$24\,519 \pm 479$	$26\,018 \pm 237$	$24\,438 \pm 470$
ζ	$1\,968 \pm 2$	$1\,807 \pm 16$	$1\,783 \pm 7$	$1\,808 \pm 8$	$1\,774 \pm 5$	$1\,805 \pm 9$
α	33.5 ± 0.4	40 ± 3	31 ± 1	30.4 ± 2	(31)	31.6 ± 2.2
β	-644 ± 25	(-648)	-644 ± 75	-492 ± 84	(644)	(-492)
γ	744 ± 26	(1 200)	(1 200)	(1 200)	(1 200)	(1 200)
M^0		(0.99)	(0.99)	(0.99)	(0.99)	(0.99)
M^2		(0.55)	(0.55)	(0.55)	(0.55)	(0.55)
M^4		(0.38)	(0.38)	(0.38)	(0.38)	(0.38)
P^2	573 (66)	(500)	(500)	(500)	(500)	(500)
P^4	524 (144)	(500)	(500)	(500)	(500)	(500)
P^6	1 173 (321)	(500)	(500)	(500)	(500)	(500)
B_0^2			$1\,096 \pm 80$	$-1\,054 \pm 117$	$-1\,108 \pm 65$	$-1\,037 \pm 137$
B_0^4		$-2\,486 \pm 170$	$1\,316 \pm 146$	$1\,146 \pm 200$	$1\,358 \pm 137$	$1\,121 \pm 303$
B_4^4			$-2\,230 \pm 85$	$-2\,767 \pm 147$	$-2\,219 \pm 76$	$-2\,948 \pm 169$
B_0^6		$-5\,287 \pm 113$	$-3\,170 \pm 379$	$-2\,135 \pm 404$	$-3\,458 \pm 267$	$-2\,120 \pm 419$
B_4^6			686 ± 246	-312 ± 227	694 ± 195	-315 ± 356
B_2^2					-78 ± 30	-77 ± 48
B_2^4					318 ± 122	356 ± 167
B_2^6					136 ± 101	158 ± 171
B_6^6					123 ± 125	424 ± 220
n	13	19	26	25	38	34
σ	10	71	36	46	39	56

Table VI. — Calculated and experimental energy levels of $ThCl_4 : U^{4+}$ in D_{2d} symmetry with the main components (in squared %) of the corresponding eigenvectors.

Γ	$E_{calc.} (cm^{-1})$	$E_{obs.} (cm^{-1})$	$\Delta E (cm^{-1})$	$g_{calc.}$	Eigenvectors (*)
4	0	0	0		89% 3H_4 + 8% 1G_4
5	148	112 (*)	36	0,49	87% 3H_4 + 9% 1G_4
1	219				80% 3H_4 + 11% 1G_4
2	805				89% 3H_4 + 9% 1G_4
1	907				88% 3H_4 + 4% 1G_4
3	986				92% 3H_4 + 8% 1G_4
5	1 144			3,50	89% 3F_2 + 9% 1D_2
3	3 821				81% 3F_2 + 16% 1D_2
5	4 000			- 1,62	76% 3F_2 + 13% 1D_2
4	4 108				85% 3F_2 + 12% 1D_2
1	4 255	4 220 (*)	35		81% 3F_2 + 13% 1D_2
3	5 706				97% 3H_5 + 2% 3F_3
5	5 810	5 815	- 5	- 0,60	93% 3H_5 + 2% 3F_2
2	5 864				96% 3H_5 + 2% 3F_3
5	6 388	6 430	- 42	0,74	95% 3H_5 + 2% 3F_2
4	6 389				95% 3H_5
5	6 609			- 6,11	94% 3H_5 + 4% 3F_2
1	6 629	6 589	40		95% 3H_5 + 2% 3F_4
2	6 693				96% 3H_5 + 4% 3F_3
4	8 424				80% 3F_3 + 7% 3F_4
5	8 476	8 470	6	5,94	91% 3F_3 + 3% 3F_4
3	8 543				91% 3F_3 + 6% 3H_6
2	8 605				82% 3F_3 + 6% 3F_4 + 6% 3H_5
5	8 677	8 666	11	- 1,07	81% 3F_3 + 5% 3F_4 + 5% 3H_6
1	8 844	8 843	1		44% 3F_4 + 39% 1G_4
5	8 991			0,26	41% 3F_4 + 33% 1G_4
3	9 041				47% 3F_4 + 26% 1G_4
2	9 297				49% 3F_4 + 31% 1G_4
1	9 441	9 405	36		55% 3F_4 + 33% 1G_4
3	9 653				56% 3F_4 + 31% 1G_4
5	9 677	9 749	- 72	3,38	51% 3F_4 + 32% 1G_4
4	10 752				83% 3H_6 + 6% 1G_4
5	10 790	10 820	- 30	1,38	86% 3H_6 + 4% 1I_6 + 4% 1G_4
1	10 803	10 752	51		93% 3H_6 + 4% 1I_6
3	11 239				90% 3H_6 + 6% 1I_6
5	11 324			1,99	90% 3H_6 + 7% 1I_6
4	11 357				87% 3H_6 + 5% 1I_6
2	11 369				92% 3H_6 + 7% 1I_6
3	11 423				88% 3H_6 + 4% 1I_6
1	11 676				86% 3H_6 + 7% 1I_6
5	11 872			- 10,19	88% 3H_6 + 6% 1I_6
3	14 650	14 610	40		52% 1D_2 + 27% 3P_2
1	14 731	14 788	- 57		31% 3P_0 + 16% 1G_4 + 14% 3F_4
4	14 854				48% 1D_2 + 38% 3P_2
5	14 939	14 928	11	- 1,89	49% 1D_2 + 33% 3P_2 + 12% 3F_2
1	15 269				31% 1D_2 + 23% 3P_2 + 22% 3P_0
1	15 397	15 388	9		37% 3P_0 + 33% 3F_4 + 22% 1G_4
5	15 566	15 529	37	0,93	47% 3F_4 + 46% 1G_4
2	15 824				52% 1G_4 + 38% 3F_4
4	15 987				50% 1G_4 + 43% 3F_4
1	16 319	16 325	- 6		50% 1G_4 + 40% 3F_4
5	16 351	16 290	61	3,01	51% 1G_4 + 42% 3F_4
3	16 703				55% 1G_4 + 38% 3F_3

Table VI (continued).

Γ	$E_{\text{calc.}} (\text{cm}^{-1})$	$E_{\text{obs.}} (\text{cm}^{-1})$	$\Delta E (\text{cm}^{-1})$	$g_{\text{calc.}}$	Eigenvectors (*)
2	17 603				94 % 3P_1 + 4 % 3F_4
5	17 847	17 804	43	- 2,98	97 % 3P_1
1	19 548				89 % 1I_6 + 8 % 3H_6
5	19 558	19 556	2	0,51	91 % 1I_6 + 8 % 3H_6
3	19 595				86 % 1I_6 + 7 % 3H_6
2	20 293				92 % 1I_6 + 7 % 3H_6
5	20 339	20 324	15	- 3,69	92 % 1I_6 + 6 % 3H_6
4	20 564				91 % 1I_6 + 5 % 3H_6
5	20 838				91 % 1I_6 + 5 % 3H_6
1	20 894				92 % 1I_6 + 5 % 3H_6
3	21 103				73 % 1I_6 + 17 % 3P_2
4	21 205				85 % 1I_6 + 6 % 3P_2
3	21 913				48 % 3P_2 + 24 % 1D_2 + 23 % 1I_6
5	22 344	22 330	14	- 2,85	62 % 3P_2 + 33 % 1D_2
1	22 647	22 669	- 22		60 % 3P_2 + 35 % 1D_2
4	22 654				50 % 3P_2 + 36 % 1D_2
1	38 406				92 % 1S_0 + 7 % 3P_0

(*) Eigenvectors are given with the percentage of each SLJ level.

(*) From fluorescence.

Table VII. — Calculated and experimental energy levels of $\text{ThCl}_4 - \text{U}^{4+}$ in D_2 symmetry with the main components (in squared %) of the corresponding eigenvectors.

Γ	$E_{\text{calc.}} (\text{cm}^{-1})$	$E_{\text{obs.}} (\text{cm}^{-1})$	$\Delta E (\text{cm}^{-1})$	Main $^{2S+1}L_J$ components
2	0	0	0	88.9 % 3H_4
3	104.0	57	47	87.7 % 3H_4
4	215.6	134	81.6	86.6 % 3H_4
1	227.3			85.9 % 3H_4
1	834.6			88.7 % 3H_4
2	938.6			84.2 % 3H_4
1	1 054.9			87.7 % 3H_4
3	1 158.4			88.8 % 3H_4
4	1 224.2			88.4 % 3H_4
1	3 826.2			80.5 % 3F_2
3	3 973.5			75.4 % 3F_2
4	4 039.3			76.3 % 3F_2
2	4 120.6			84.8 % 3F_2
1	4 272.1			80.4 % 3F_2 + 12.5 % 1D_2
1	5 712.6			96.7 % 3H_5
4	5 804.7			84.6 % 3H_5
3	5 814.6	5 815	- 0.4	78.6 % 3H_5
2	5 866.2			95.6 % 3H_5
2	6 370.9	6 412	- 41.1	83.7 % 3H_5
4	6 430.6			93.5 % 3H_5
3	6 469.7	6 524	- 54.3	82.5 % 3H_5
4	6 600.3			82.7 % 3H_5
3	6 655.5	6 589	66.5	93.5 % 3H_5
1	6 698.3			85.3 % 3H_5
2	6 732.7			94.1 % 3H_5

Table VII (continued).

Γ	$E_{\text{calc.}} (\text{cm}^{-1})$	$E_{\text{obs.}} (\text{cm}^{-1})$	$\Delta E (\text{cm}^{-1})$	Main $2S+1L_J$ components
3	8 419.5			77.7 % ³ F ₃
4	8 433.1			86.2 % ³ F ₃
1	8 520.3			91.4 % ³ F ₃
2	8 541.5			90.2 % ³ F ₃
2	8 616.4			78.3 % ³ F ₃
3	8 672.1	8 628	44.1	77.3 % ³ F ₃
4	8 699.4	8 705	- 5.6	73.8 % ³ F ₃
1	8 828.3	8 843	- 14.7	43.1 % ³ F ₄ + 23 % ¹ G ₄
3	8 960.1			29.8 % ³ F ₄ + 23.6 % ¹ G ₄
4	9 009.8			29.4 % ³ F ₄ + 23.8 % ¹ G ₄
2	9 035.9			39.4 % ³ F ₄ + 24.4 % ¹ G ₄
2	9 308.5			48.4 % ³ F ₄ + 30.6 % ¹ G ₄ + 11.4 % ³ F ₃
1	9 450.8	9 405	45.8	55.2 % ³ F ₄ + 32.8 % ¹ G ₄
1	9 670.7			55.8 % ³ F ₄ + 30.8 % ¹ G ₄
4	9 697.8	9 737	- 39.2	50.4 % ³ F ₄ + 21.6 % ¹ G ₄
3	9 707.2	9 762	- 54.8	32.8 % ³ F ₄ + 20.6 % ¹ G ₄
2	10 750.7			81.3 % ³ H ₆
1	10 771.4			84.3 % ³ H ₆
3	10 809.9	10 752	57.9	91.8 % ³ H ₆
4	10 822.2	10 820	- 2.2	82.3 % ³ H ₆
1	11 268.4			88.4 % ³ H ₆
3	11 293.7			83.7 % ³ H ₆
4	11 373.2			76.1 % ³ H ₆
2	11 416.2			78.9 % ³ H ₆
1	11 437.2			79.5 % ³ H ₆
2	11 459.8			83.4 % ³ H ₆
1	11 751.1			81.7 % ³ H ₆
3	11 883.6			80.3 % ³ H ₆
4	11 950.8			74.3 % ³ H ₆
1	14 630.3	14 608	22.3	40.2 % ¹ D ₂ + 20.8 % ³ P ₂
2	14 735.6	14 787	- 51.4	21.6 % ³ P ₀ + 13.4 % ¹ D ₂ + 10 % ³ P ₂
1	14 874.9	14 800	74.9	47.4 % ¹ D ₂ + 38 % ³ P ₂
4	14 886.0	14 872	- 14	47.4 % ¹ D ₂ + 31 % ³ P ₂
3	14 980.5	14 975	5.5	49 % ¹ D ₂ + 33.2 % ³ P ₂
1	15 256.6			30.5 % ¹ D ₂ + 23 % ³ P ₂ + 19.5 % ³ P ₀ + 9.5 % ¹ G ₄
1	15 393.5	15 399	- 5.5	41.5 % ³ P ₀ + 24.1 % ³ F ₄ + 17.9 % ¹ G ₄
3	15 526.8	15 528	- 1.2	46.8 % ³ F ₄ + 27.8 % ¹ G ₄
4	15 552.7	15 538	14.7	31 % ³ F ₄ + 29.4 % ¹ G ₄
2	15 816.5			51.6 % ¹ G ₄ + 37.8 % ³ F ₄
1	15 951.5			49.8 % ¹ G ₄ + 42.8 % ³ F ₄
2	16 320.4	16 282	38.4	50 % ¹ G ₄ + 25.4 % ³ F ₄
4	16 332.0	16 325	7	47 % ¹ G ₄ + 38.4 % ³ F ₄
3	16 412.0	16 303	109	33.2 % ¹ G ₄ + 26 % ³ F ₄
1	16 727.8			52.2 % ¹ G ₄ + 35.6 % ³ F ₄
2	17 632.7	17 675	- 42.3	93.1 % ³ P ₁
4	17 829.2	17 789	40.2	97.4 % ³ P ₁
3	17 878.3	17 814	64.3	97.3 % ³ P ₁
1	19 549.4			83.3 % ¹ I ₆
3	19 551.3	19 541	11.7	86 % ¹ I ₆
4	19 579.5	19 572	8.5	88.8 % ¹ I ₆
1	19 607.6			81.1 % ¹ I ₆
4	20 266.4			82.3 % ¹ I ₆
2	20 292.6			84.7 % ¹ I ₆
3	20 478.1			88.9 % ¹ I ₆

Table VII (continued).

Γ	$E_{\text{calc.}} (\text{cm}^{-1})$	$E_{\text{obs.}} (\text{cm}^{-1})$	$\Delta E (\text{cm}^{-1})$	Main $2S+1L_J$ components
2	20 657.6			81.6 % 1I_6
3	20 860.7			92 % 1I_6
4	20 939.1			87.9 % 1I_6
1	20 986.8			89.2 % 1I_6
1	21 144.2			50.2 % 1I_6
2	21 231.4			82.8 % 1I_6
1	21 914.1			46 % 3P_2 + 23 % 1I_6 + 22.6 % 1D_2
4	22 307.4	22 280	27.4	60 % 3P_2 + 32.5 % 1D_2
3	22 386.7	22 330	56.7	62 % 3P_2 + 33.2 % 1D_2
1	22 653.5	22 705	51.5	58.6 % 3P_2 + 34.8 % 1D_2
2	22 695.2			48.8 % 3P_2 + 35.6 % 1D_2
1	38 358.8			92.4 % 1S_0

can be introduced to measure the relative strength of the crystal field and table VIII shows their values for different compounds. $\text{ThCl}_4 - \text{U}^{4+}$, as $\text{ThBr}_4 - \text{U}^{4+}$ [1] is a system with a relatively weak crystal field, in comparison to $\text{U}(\text{BD}_4)_4$ [2] or Cs_2UCl_6 [18], and this results in a fitting with a reasonably small r.m.s. despite of the modulation of the matrix and the approximate symmetry D_{2d} used for U^{4+} in ThCl_4 . In the one hand, this weakness of the crystal field in $\text{ThX}_4 - \text{U}^{4+}$ was a favourable element that permitted us to use the parameters of $\text{ThBr}_4 - \text{U}^{4+}$ [1] as starting values in view of the similarity of the spectra of U^{4+} in the tetrachloride and the tetrabromide. But on the other hand, instead of enhancing the possible variations from a bromide host to a chloride, the parameters in both hosts showed no systematic trend, whereas there is a clear decrease in the values of the free ion F^k parameters for U^{4+} in borohydrides [2] compared to those in the thorium tetrahalides, which is due to covalent character of the hydrogen (deuterium) — uranium bond compared to the much more ionic halide-uranium one.

Table VIII. — Values of the Auzel parameter for U^{4+} in different compounds (in cm^{-1}).

	$\text{ThCl}_4 - \text{U}^{4+}$	$\text{ThBr}_4 - \text{U}^{4+}$	$\text{U}(\text{BD}_4)_4$	Cs_2UCl_6
$\frac{N_v}{\sqrt{4\pi}}$	1 560	1 544	3 942	3 325

6. Conclusions.

The optical spectra of $\beta - \text{ThCl}_4 - \text{U}^{4+}$ represent with $\beta - \text{ThBr}_4 - \text{U}^{4+}$ [1] the only cases of an optically active ion U^{4+} ($5f^2$) fully studied in an incommensurately modulated structure. The spectroscopic identification of lines corresponding to U^{4+} in sites of S_4 (approximated by D_{2d}) and D_2 symmetries permitted us to propose a parametric analysis of U^{4+} in both symmetries. The results, comparable to those obtained for $\text{ThBr}_4 - \text{U}^{4+}$ do not exhibit a systematic trend in the values of the parameters in passing from the bromide to the chloride. This fact could come from the relatively large deviations from the crystal field model for the actinides that would hide this effect when the coordination polyhedra of the actinide are too similar.

References

- [1] DELAMOYE, P., RAJNAK, K., GENET, M., EDELSTEIN, N., *Phys. Rev. B* **28** (1983) 4923.
- [2] RAJNAK, K., GAMP, E., SHINOMOTO, R., EDELSTEIN, N., *J. Chem. Phys.* **80** (12) (1984) 5942.
- [3] BERNARD, L., CURRAT, R., DELAMOYE, P., ZEYEN, C. M. E., HUBERT, S., DE KOCHKOVSKY, R., *J. Physique. C* **16** (1983) 433.
- [4] DELAMOYE, P., BERNARD, L., CURRAT, R., KRUPA, J. C., PETITGRAND, G., Communication at the conference « Journées de l'état solide », Bordeaux, France, June 1984.
- [5] DELAMOYE, P., CURRAT, R., *J. Phys. Lett.* **43** (1982) L-655.
- [6] KRUPA, J. C., KHAN MALEK, C., DELAMOYE, P., MOINE, B. and PEDRINI, C., to be published.
- [7] HUSSONNOIS, M., KRUPA, J. C., GENET, M., BRILLARD, L., CARLIER, R., *J. Crystal Growth* **51** (1981) 11.
- [8] MOONEY, R. C. L., *Acta Cryst.* **2** (1949) 189.
- [9] MASON, J. T., JHA, M. C., CHIOTTI, P., *J. Less. Commun. Metals* **34** (1973) 143.
- [10] KHAN MALEK, C., KRUPA, J. C., to be published.
- [11] KOSTER, G. F., DIMMOCK, J. O., WHEELER, R. G., STATZ, H., *properties of the thirty two point groups* (M. I. P. Cambridge Mass) 1963.
- [12] ESTEROWITZ, L., BARTOLI, J. F., ALLER, R. E., WORTMAN, D. E., MORRISON, C. A., LEAWITT, R. P., *Phys. Rev. B* **19** (1979) 6442.
- [13] BRIAT, B., DELAMOYE, P., RIVOAL, J. C., HUBERT, S., EVESQUE, P., *J. Physique* **46** (1985) 1375.
- [14] GENET, M., DELAMOYE, P., EDELSTEIN, N., CONWAY, J., *J. Chem. Phys.* **67** (1977) 1620.
- [15] FLINT, C. D., TANNER, P. A., *Mol. Phys.* **53** (1984) 429.
- [16] HUFNER, S., *Optical spectra of transparent rare earth compounds* (Academic press, N. Y.) 1978.
- [17] AUZEL, F., MALTA, O. L., *J. Physique* **44** (1983) 201.
- [18] JOHNSTON, D. R., SATTEN, R. A., WRONG, E., *J. Chem. Phys.* **44** (1966) 687.
- [19] VAN DEURZEN, C. H. H., RAJNAK, K., CONWAY, J. G., *J. Opt. Soc. Am. B* **1** (1984) 45.